A simple design of uniform LED illumination using catadioptric collimator and freeform lenslet array

DT Vu PhD[a] , **H Vu** MSc[b], **S Shin** PhD[b], **NM Kieu** BSc[c], **TQ Tien** PhD[c] and **NH Vu** PhD[a]

[a]Faculty of Electrical and Electronics Engineering, Phenikaa University, Hanoi, Vietnam
[b]Department of Information and Communication Engineering, Myongji University, Gyeonggi-do, Korea
[c]Institute of Material Science, Vietnam Academy of Science and Technology, Hanoi, Vietnam

We introduce a compact lenslet array principle that takes advantage of freeform optics to deploy a light distributor, beneficial for highly efficient, inexpensive, low energy consumption light-emitting diode (LED) lighting system. We outline here a simple strategy for designing the freeform lens that makes use of an array of the identical plano-convex lenslet. The light is redistributed from such lenslet, hinging on the principle of optical path length conservation, and then delivered to the receiver plane. The superimposing of such illumination area from every lenslet occurs on the receiver plane, in which the non-uniform illumination area located in the boundary should have the same dimension as the size of the freeform lenslet array. Such an area, insofar, is negligible due to their small size, which is the crux of our design, representing a large departure from the former implementations. Based on simulations that assess light performance, the proposed design exhibited the compatibility for multiple radiation geometries and off-axis lighting without concern for the initial radiation pattern of the source. As simulated, the LED light source integrated with such proposed freeform lenslet array revealed high luminous efficiency and uniformity within the illumination area of interest were above 70% and 85%, respectively. Such novel design was then experimentally demonstrated to possess a uniformity of 75% at hand, which was close to the simulation results. Also, proposed indoor lighting was implemented in comparison with the commercial LED downlight and LED panel, whereby the energy consumption, number of luminaires and illumination performance were assessed to show the advantage of our simplified model.

1. Introduction

Over the past decades, light-emitting diodes (LEDs) have advanced rapidly and emerged as a promising candidate for future light-emitting devices because of their high luminous efficiency, low energy consumption, long lifespan, fast switching, eco-friendly and compactness.[1–6]

Address for correspondence: NH Vu, Faculty of Electrical and Electronics Engineering, Phenikaa University, Yen Nghia, Ha Dong, Hanoi 12116, Vietnam.
E-mail: hai.vungoc@phenikaa-uni.edu.vn

With the rapid progress of technology, the highly efficient LEDs are becoming more affordable, which helps increasingly performance- and cost-competitive to other forms of traditional light sources.[7–9] Nonetheless, there are technological constraints to model LED illumination, in comparison with the conventional counterpart, owing to the inhomogeneous radiation distribution types of LEDs such as Lambertian, batwing and side-emitting patterns.[10–12] To that end, such LED sources are impractical for lighting in many contexts such as indoor lighting, automotive lighting, tunnel lighting and street lighting, where have most often required a uniform illumination. Therefore, undoubtedly, one of the major trends in the field of LEDs research is to develop diverse geometries of the uniform illumination pattern as well as the compact design of the lighting system. To do this, the optical components have been broadly used to redistribute and reshape LEDs illumination pattern. It is known that the design of the optical component for LEDs mainly based on optimising the radiation transfer from a source to a target. Among all the optical components, the freeform surfaces can provide the advantages such as high degree of design freedom, compact size and accurate light pattern control (shape, uniformity, intensity, etc.), thereby making it the most widely used optical component in LED illumination.[10,13] Various methods for designing freeform lenses have been developed; however, the calculation for freeform optical surface usually arises to a first-order partial differential equation[13] or second-order nonlinear partial differential equation of the Monge–Ampère type.[14] In parallel, Benítez's group developed the simultaneous multiple surface (SMS) method to design simultaneously two freeform surfaces for optical components,[15] which was more advantageous to control the light rays compared to single freeform surface design. Another study using ray mapping approach to design a total internal reflection (TIR) lens obtained the highly uniform illumination distribution up to approximately 90%, ideally.[16] However, in those studies, in addition to the mathematical complexity in the calculation, the designs for the freeform optical components were only feasible for certain radiation distribution of the LED source. This is because the specific parameters of the lens surface strongly depend on the position, intensity distribution and emitting direction of the LED, making the manufacture a very delicate task. In other words, those methods have been restricted to use for multiple LED sources.

Because they are free from such issues, the method using a secondary optical component based on freeform optics principle is particularly interesting to deploy in the LED lighting system. This clever design not only results in uniform distribution of illumination pattern but also is well suited for multiple LED radiation patterns. Recent developments taking advantage of this design have brought a new dimension to the highly efficient LED lighting. Wang et al. investigated that a combination of a Fresnel lens and a microlens array could produce multiple shapes of illumination distribution.[17] In their design, the Fresnel lens and microlens array were used as a collimator and distributor, respectively, which helped to control the shape and uniformity of the illumination area with no restriction on the LED sources. Hai and co-workers showed that a uniform LED lighting system could be easily obtained by designing simple secondary optics components.[18] In this model, an array of collimators, made up of plano-convex lenses, worked for collimation and a contributor comprising of a pair of Fresnel lens worked for redistributing the collimated beam on two dimensions in the desired area. Using TIR lenses combined with double Fresnel lenses, our group also achieved a uniform illumination distribution in a lighting area of interest.[19] A combination of a thin lens and a freeform surface was also proposed to tackle along this avenue, in the spirit of uniform LED irradiation.[20,21] These aforementioned efforts demonstrated that the strategy using a secondary optical component is advantageous for the LEDs lighting system especially in term of illumination performance and compatibility to various types of the LED light sources. Still, these studies have to

design individually for each component to acquire the spatial uniformity of flux distribution, whereby arising to the relative complexity of the manufacturing process for such a secondary optical component. Besides, another drawback of such former studies[18,19] was the significant optical loss due to the use of two surfaces of secondary optics for redistributing of light. Those works provided an excellent driven for the alternative approach based on the coincide of illumination area from all identical plano-convex lenslet of a freeform lenslet array, described below.

This work exploits a simple and robust optical design for LED lighting system containing a collimator and a freeform lens array to control the distribution and shape of the LED illumination area. Herein, a TIR collimator was employed for the purpose of collimating LED light. The freeform lens was constructed based on an array of identical plano-convex lenslets to redistribute the collimated beam to an illumination area. We propose a design principle of lenslet based on the conservation of optical path length and reasonably predict the coincide of uniform radiation from every lenslet in the illumination area. Fortunately, non-uniform illumination area is not too acute an issue because of its small size, which has the same dimension as the freeform lenslet array in principle (we describe in more detail in section 2.2). The key advantages for synergy between the TIR collimator and the freeform plano-convex lenslet array are as follows: (i) the optical components are straightforwardly designed through geometry optics and non-imaging optics principle, which can get rid of solving complex partial differential equations, (ii) the TIR collimator is generally compatible with the radiation distribution of multiple LED sources, making them widely used for the LED lighting system, (iii) the radiation distribution of LED light can be easily tuned by varying the structure of the freeform lenslet array and (iv) such design of the freeform lenslet array is also advantageous for off-axis illumination.

2. System design

Figure 1 shows the schematic diagram of the LED lighting system developed in this work. It contains, from left to right, a commercial LED light source, a TIR collimator and a freeform lenslet array composed of the identical plano-convex lenslet. Let us give more optical-related features for the setup, shown in Figure 1: an output LED beam is first collimated by using a TIR collimator (i.e., TIR catadioptric lens type). The collimated beam is then redistributed by a freeform lens array and delivered to an illumination area. In fact, the output beam after collimation is not an ideal parallel beam because the LED source is regarded as a collection of the series of point sources. In addition, the collimated beam has an intensity distribution of the Gaussian lineshape, causing a rapid decay with emission angle. To alleviate this, we can recourse to the freeform lenslet array, where the collimated beam can be viewed as an assembly of distinct rays. In each individual lenslet, the illumination area can be assumed to have a uniform distribution. We defer the detailed optical and parameter figure of merit for further discussion and will present below the optical principle verified with the simulation and experimental results.
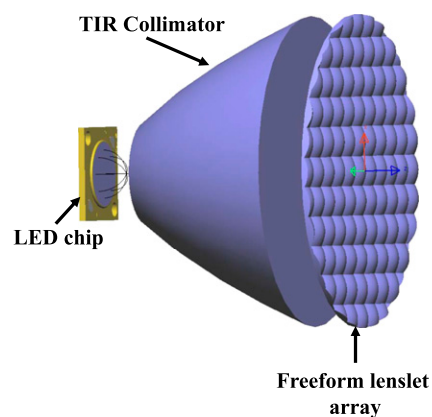
Figure 1   Schematic diagram of LED lighting system. It contains an LED chip, a TIR collimator and a freeform lenslet array composed of plano-convex lenslet
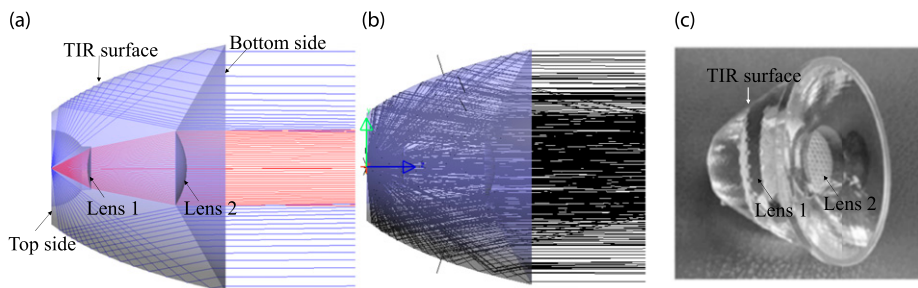
2.1 Collimator

In this study, the collimator was used for the purpose of collecting and then deflecting the rays emitted from the LED source to become a collimating beam. As a proof-of-concept, we utilised a mature design of a TIR catadioptric lens serving as a collimator, comprising of a TIR surface and a pair of refractive lenses,[19] as shown in Figure 2(a). The former collects the light from the wide-angle, while the latter is responsible for the small-angle light rays. The second lens is placed at the focal point of the first counterpart, aiming to produce a collimating output beam. Technically, the catadioptric lens works well on an ideal point source; however, we here also prove its effectiveness to an LED chip to produce a parallel output beam. To cross-check the deviation of the beam, the ray traces for point source and the LED chip were investigated. The LightTools[TM] program (version 8.4) was employed to trace a collection of light rays emitted from the light source through the TIR collimator and analysed by geometrical optics method, which readily allows in-depth performance analysis of the light beam.

Figure 2(a) and (b) illustrate the ray traces from a point source and an LED chip, respectively. In this simulation, the TIR collimator possesses specifications same as the commercial catadioptric lens (Led-link Optics Inc.) as shown in Figure 2(c). The diameters of the top and bottom sides of the collimator were 30 and 75 mm, respectively. Figure 2(a) clearly displays that the light rays from the point source could be collimated perfectly by this collimator. The blue and red rays present the lights collimated by the TIR surface and two refractive lenses, respectively. One should keep in mind that a tiny portion of light emitted from the LED would be reflected at the side of the holder of the lens and thus deviated from the collimating beam, as can be seen in the green stray rays in Figure 2(a). Such TIR collimator was also possible to expect to work well with an LED source to produce an output collimating beam. To assess the degree of collimating for LED source, we implemented the simulation with a 10 mm diameter LED chip. Figure 2(b) exhibits the ray-tracing of light after passing through the TIR collimator, which indicates that the output beam was almost parallel. To evaluate a precise collimating performance, we must analyse the output beam size at two distinct positions on the ray path. Such an analysis of widening of beam exhibited an output beam divergence of 7.5°, still would be entirely suitable for common illumination purpose. This phenomenon is attributed to the non-ideal point source nature of the LED light. We thus point out that the output beam holds relatively small divergence, which is a good starting point for our further study of designing the freeform lenslet array.

2.2 Light distributor

Although the collimated beam was created in the previous simulation, they were still not


Figure 2   Model of the TIR collimator integrated with (a) a point source, (b) an LED source and their corresponding rays diagram and (c) photograph of a TIR collimator

uniform fashion, which is the main issue for many contexts in practical application. To address this issue, a distributor is needed to implement the mandatory redistribution of the collimated light. It is well known that the light distributor usually works on refraction or reflection principles, in several innovative fashions.[9,10,13-19] Most design of the light distributor often has to implement for each individual element, thereby increasing the complexity in the manufacturing process. A mitigation of such complexity is to use the same identical optical element. We here propose along this line a light distributor principle consisting of an array of the freeform plano-convex lenslet. The collimated beam is divided into smaller regions and we thus reasonably assume that the luminous intensity distribution within each individual lenslet can be regarded in a uniform fashion. After redistributing by the lenslet, the radiation beam is subsequently delivered to the receiver plane and superimposed with each other at here. It is thus expected that the proper design of a freeform lens array composed of the plano-convex lenslet may render the distribution of the collimated beam uniform and extended. In the geometry of Figure 3(a), there would be, of course, two distinct illumination areas: a uniform area located at the centre and two boundaries at the side of the illumination pattern as can be intuited. The former is associated with the coincide of multiple illumination areas and the latter is contributed only from the radiation of the outermost lenslet. The size of these boundaries (S) has the same dimension as that of the freeform lenslet array. So, as shown in Figure 3(a), we can expect that this non-uniform illumination area is very secondary in principle. This lead to an insignificant change in the uniformity of the illumination area of interest on the receiver plane, as we will see more detail in the experimental results section. By the same token, we believe that our simple design has some heuristic interest, on the one hand, illumination area is spread on the receiver plane, on the other hand, radiation distribution is highly uniform, over 70% at least (we will provide a corresponding result below).

Next, we assess the ray-tracing analysis of the freeform lenslet array as the schematic diagram illustrated in Supplemental Figure 1(a). This freeform lens contains a 2D array of the square plano-convex lenslet. Such single lenslet typically is designed with small size, a couple of 1's of mm. We indicate the number of the lenslet in a row (N) in Supplemental Figure 1(a) and will report on how this factor affect to the light performance (see below in Section 3). We assume here that the distance from the collimator to the target surface is much larger than the size of the collimator and the freeform lenslet array. Superimposing all the redistributed uniform radiation, as discussed above, on the illumination area from every lenslet, the final distribution could be obtained on the receiver, as shown in Supplemental Figure 1(a). Such an optimal design can be favourably traded-off of the thickness and number of single lenslet and the ability for mass production. Coarsely speaking, for such given freeform lens array, the reduction of the thickness of the single plano-convex lens would lead to the increase of the size of the freeform lens and bring to an improvement of uniformity, while the manufacturing process would be more complex and vice versa.[18,19] Similarly, the single plano-convex lenslet also could redistribute the narrow collimated beam in a two-dimensional area on the receiver (see Supplemental Figure 1(b)). To this end, we can hope a uniform illumination distribution if a proper structure design of the freeform lens is employed.

Let us now describe the main characteristics of Figure 3(b) that we sketch the geometrical optics as a proof-of-principle of the freeform lenslet. A typical plano-convex lens is composed of one convex surface and one flat surface. Figure 3(b) displays the representative cross-section of a plano-convex lens. For simplicity, we consider that the collimated beam passing through the plano-convex lens is focused at a focal point (F) and then spread on a receiver plane, hereafter referred to as RR'. All in all, in this simulation, all the rays travelling through the lens to a focal point has equal optical path length (OPL), obeyed the
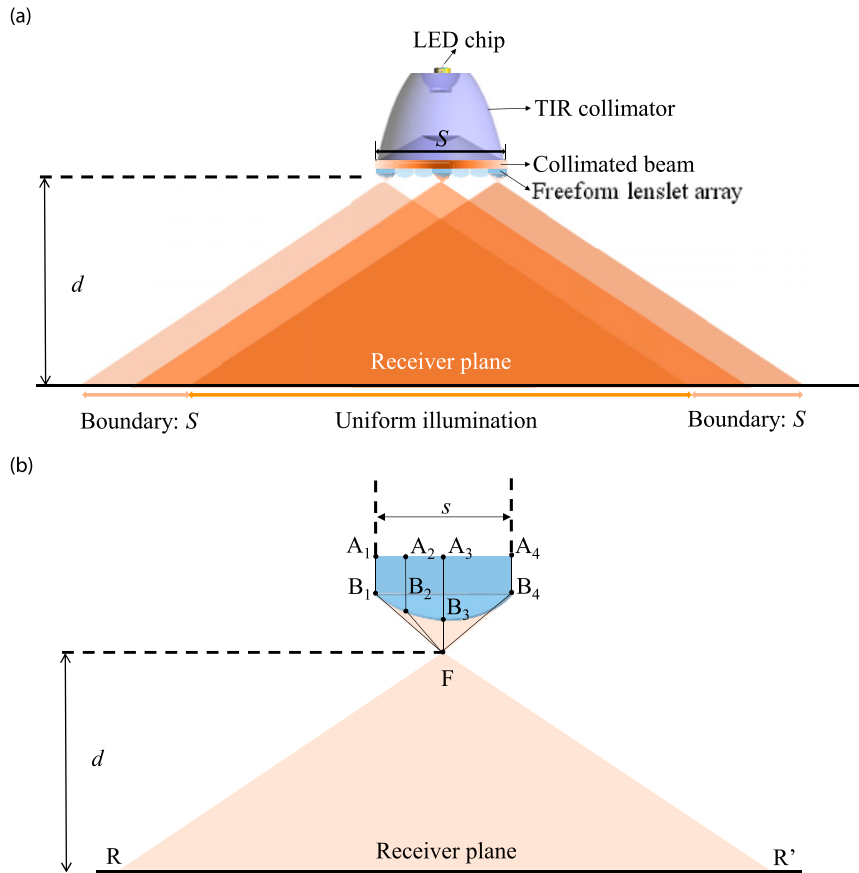
Figure 3 (a) Lateral cross-section and ray diagram of the propsed LED lighting system indicating highly uniform illumination at the centre and two non-uniform illuminations at the boundary of illumination pattern on the receiver plane. Note that the size of the freeform lenslet array was enlarged to ease envisioning. (b) Lateral cross-section and ray diagram of freeform plano-convex lenslet to generate the uniform illumination on a receiver plane. Note that the size of the freeform lenslet was enlarged to ease envisioning

law of optical path length conservation. We further assume here that all incident rays are parallel and normal to the flat surface of the plano-convex lens. Two outermost rays, that is, A_1B_1 and A_4B_4, are deflected and intersect the receiver plane at R' and R, respectively. All of the other rays will also be focused at F, and then lie within the receiver plane (RR'). Therefore, the optical path length can be written as a sum of the geometrical lengths of the rays travelling in lens and air for several typical cases, for instance, according to equation (1)

$$
\begin{aligned}
n_1|A_1B_1| + n_0|B_1F| &= n_1|A_2B_2| + n_0|B_2F| \\
&= n_1|A_3B_3| + n_0|B_3F| \\
&= n_1|A_4B_4| + n_0|B_4F|
\end{aligned}
$$

$$(1)$$

where n_0, n_1 are the refractive indices of air and lens material, respectively. A_nB_n ($n = 1$–4) and B_nF ($n = 1$–4) are the geometrical lengths of the rays travelling in lens material and air medium, respectively, as indicated in Figure 3(b).

We then used an ad hoc program written in Matlab to treat mathematically equation (1) for all coordinates of the segment surface curve. We would thus obtain an entire profile of the surface shape of the plano-convex lenslet to produce the uniform illumination in a two-dimensional receiver. A 3D cross-section version of a plano-convex lenslet, as shown in Supplemental Figure 1(b), was then obtained in the 3D modelling software (LightTools™) for ray-tracing study.

Supplemental Figure 2 shows the flowchart to determine the proper structural design of the freeform plano-convex lens array. We started by selecting the appropriate size of the freeform lenslet array to adapt that of the TIR collimator (75 mm diameter). The size of lenslet was then straightforward deduced at a preset fixed number of lenslet in a row (N). The initial parameters such as the size of lenslet array (s), the refractive index of lenslet material ($n = 1.49$), distance from the light source to the receiver (d) and the size of the receiver (RR') were subsequently used to determine the focal point of a plano-convex lenslet. Such input parameter (s, n, d, RR') was purposely selected to trace the 3D coordinate of the lens surface. Specifically, d and RR' was selected to grant a uniform illumination in a 1.5×1.5 m receiver located at 2 m away from the lenslet array. We stuck an effective refractive index of PMMA, $n = 1.49$ in our calculation. The size of each lenslet (s) was changed, pertaining to the number of lenslets (N) to optimise the optical efficiency and uniformity of our proposed LED. By using an ad hoc program written in Matlab to calculate the equation (1), the 3D coordinates of the surface curve were found. This process could be repeated to determine an appropriate design for the freeform lenslet array with a different number of the lenslet in a row. A stream of data for these structural parameters, that is, 3D coordinates of the surface curve of single lenslet, would be extracted for further simulation study using LightTools™ software to assess the uniformity and efficiency of the radiation pattern. Finally, the freeform lenslet array was straightforwardly constructed by replicating and translating the plano-convex lenslet in two dimensions.

In another variant, in order to produce the multiple shapes of illumination distribution, we modified an original square geometry of the flat surface of a plano-convex lens. We see that if we choose a lenslet geometry capable of the close-packed arrangement in a 2D array, we can acquire any desired illumination shape. To do this, the lenslet has to be arranged in a 2D surface with no overlaps and no gaps in between. As illustrated in Supplemental Figure 3(a)–(c), we observed the transitions of illumination configurations on the receiver plane with three geometries of lenslet, that is, square, rectangle and hexagonal. For an off-axis configuration of illumination, an asymmetry geometry of plano-convex lenslet was designed with the purpose of tuning its focal point away from its centre, aiming to move the illumination area to any desired region. So, the alternative version for the lenslet of the off-axis lighting, comprised of a flat surface and a convex asymmetry counterpart, can be straightforwardly deduced (see Supplemental Figure 3(d)).

3. Simulation results

The LightTools™ simulation was employed to assess the optical features of the illumination area in our proposed LED lighting system. Figure 4 is the schematic diagram of the system using the TIR collimator + lenslet array to produce a square uniform illumination on a receiver plane. Note that the size of the freeform lenslet array with a diameter of 75 mm was enlarged to ease envisioning. The collimating beam was redirected and uniformly distributed in a 1.5×1.5 m receiver located at 2 m away from the lenslet array. Table 1 presents all the design parameter for our proposed lighting system. Polymethyl methacrylate (PMMA, $n = 1.49$) is usually material-of-choice for moulding technique owing to its high flexibility, easy fabrication features, excellent mechanical strength, chemical and physical stability.[22] In addition, they have high optical transparency and low-cost, making them an excellent candidate for designing optical components.

Efficiency and uniformity are key characteristics of lighting performance. The uniformity of
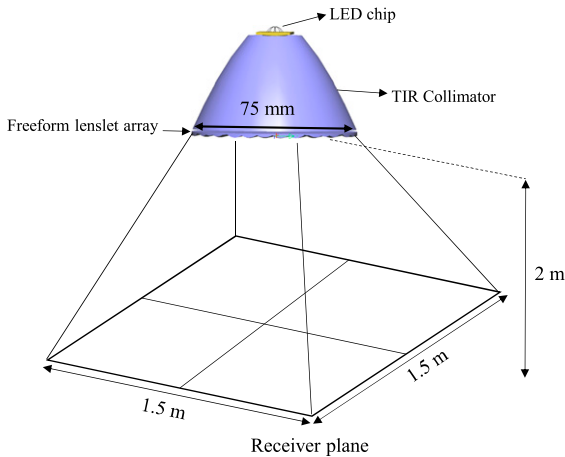
Figure 4 Illustration of the propsed LED lighting system to produce the uniform illumination on a receiver plane. Note that the size of the freeform lenslet array with a diameter of 75 mm was enlarged to ease envisioning

Table 1 The design of our proposed lighting system

Design parameters	Value
Diameter of lenslet array	75 mm
Number of lenslet in a row (N)	7, 8, 9, 10, 11
Thickness of lenslet array	5 mm
Refractive index of lenslet material (n)	1.49
Size of receiver plane (s)	1.5 × 1.5 m
Distance from light source to receiver plane (d)	2 m

illumination area (U) is calculated from the ratio of the minimum illumination (I_{min}) and average illumination (I_{avg}) using equation (2)[18,19]

$$U = \frac{I_{min}}{I_{avg}} \qquad (2)$$

Optical efficiency (OE) is defined as the ratio of light energy incident on the receiver to light energy exiting from the light source, according to equation (3)[23,24]

$$OE = \frac{Flux\ on\ Receiver}{Flux\ of\ LED\ source} \times 100\% \qquad (3)$$

where the luminous flux on the receiver and luminous flux of the LED source was determined by LightTools™ software. It was anticipated that the illumination performance of LED light would be strongly influenced by varying the key structural parameter, for example, the number of freeform lenslet in a row (N). Supplemental Figure 4 displays the dependence of the efficiency and uniformity on N. The simulation result indicates that uniformity increased with the number of the freeform lenslet in a row. In contrast, it also clearly displays that the efficiency of illumination decreased upon an increasing number of the lenslet in a row. According to the simulation results, the optimised number of lenslet was 9. However, we choose here the number of lenslet in a row of 7, still would have high uniformity and efficiency (we just lose 1.5% in light uniformity compared to the use of nine lenslet), which could solve the cost and complexity issue for the manufacturing process.

To examine the compatibility of different types of LED sources with the proposed lighting system, we studied the illumination performance of two LED lights, that is, Cree white (Xlamp XB-D, Supplemental Figure 5(a) and (c))[25] and Chip-on-broad (CoB, CXA LED array, Supplemental Figure 5(d) and (f))[26] with the same power of 10W. In the technology landscape, CoB array can capitalise to integrate many chips on a circuit board that change the amount of radiation power drastically, compared to compact discrete LEDs. Still, their size would become somewhat larger, whereby reducing the uniformity of radiation pattern, in comparison with the Xlamp XB-D LED family. Supplemental Figure 5(b) and (e) show that the intensity distribution of the CoB LED has a Lambertian pattern, whereas that of Cree White LED is non-Lambertian. The details for both LED lights can be found in Table 2. The total flux was 250 lm for both types of LED lights. In this simulation, the distance from light source to receiver plane (d) and the size of receiver plane (RR') was kept the same as those shown in Figure 4. The simulation results of the light

Table 2 The parameters of Cree white and CoB white LED lights

Parameters	Cree white	CoB
Intensity distribution	Non-Lambertian	Lambertian
Maximum wavelength peak (nm)	630	630
Luminous flux (lm)	250	250
Diameter of LED light (mm)	3	12

distribution of both LED lights integrated with the proposed lighting system on the receiver are displayed in Figure 5(a) and (b). As anticipated, the light distribution of Cree white light was more slightly uniform than that of CoB counterpart (specifically 83 vs. 80%). It is likely that the size of Cree white light is smaller compared to the CoB counterpart, making it easy-redistributing using the collimator + the light distributor. However, the uniformity of the illumination area using the CoB light was still well for standard lighting. In addition, the angular intensity distributions of those LED chips integrated with the proposed lighting system were investigated and shown in Figure 5(c) and (d). Compared to those of Supplemental Figure 5(b) and (e), it exhibits that the divergent angle of both LED sources was reduced from ±120° to ±40° that facilitates light delivering as much as possible to the illumination area of interest. It is known that most of the high power LED is based on mature CoB technology (whose performances are nowadays very good). Although the high power LED is generally difficult to redistribute uniformly, our proposed design showed that it indeed worked well for CoB LED. We finally choose CoB white LED for the next investigation because of its high radiation power, which is beneficial for the practical lighting application.

The positive point of our design is that it shows the concept feasibility for producing the various illumination shapes on the receiver area. Beside the square pattern, we can dream of an illumination area with the other patterns, e.g., rectangle and hexagon. To obtain this, we tailored the design of the single lenslet to the aforementioned shapes. Figure 6(a) and (b) present the light distribution for rectangular and hexagonal lenslet, respectively. The uniformity and efficiency of the rectangular illumination area were determined to be about 75 and 85%, respectively, in an area of 0.75×1.5 m, as revealed in Figure 6(a). The corresponding values for the hexagonal illumination area with the base edge length of 0.8 m, obtained from Figure 6(b), were 70 and 86%. The inevitable loss of optical efficiency is due to Fresnel loss and geometrical loss,[18] which lies in our prediction. Thus this can be neglected and we indeed proved that these clever designs can produce desired radiation patterns in the illumination area without concern for the initial emission patterns of the LED sources.

Our design is also expected to allow off-axis lighting that likely benefits for various purposes of lighting. Supplemental Figure 6(a) and (b) present the on-axis and of axis lighting, respectively. The concept of the on-axis and off-axis lighting relates to the relative position of the light source to the illumination area.[17,18] The former involves the lighting that the light source is above the centre of the illumination area. The latter relates to the light source out of centre of illumination. One possible design for off-axis lighting is the combination of a flat surface and a convex asymmetry counterpart, capable of moving the focal point away from the centre of a lenslet. Technically, we first selected a certain focal length, followed by designing the texture of lenslet by solving the equation (1) to determine the corresponding surface curve. The light distribution of radiation pattern for off-axis configuration is shown in
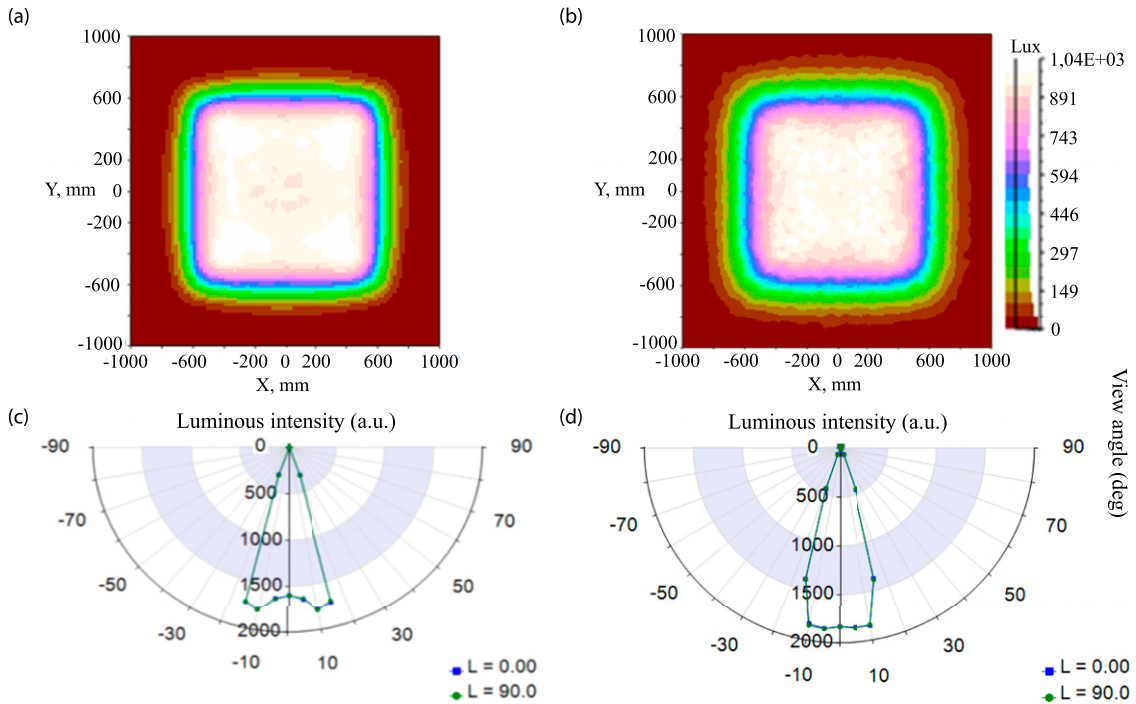
Figure 5   Light distributions on a receiver plane using TIR collimator + freeform square lenslet array integrated with: (a) Cree white LED, (b) CoB white LED. Angular intensity distributions of (c) Cree white LED, (d) CoB white LED
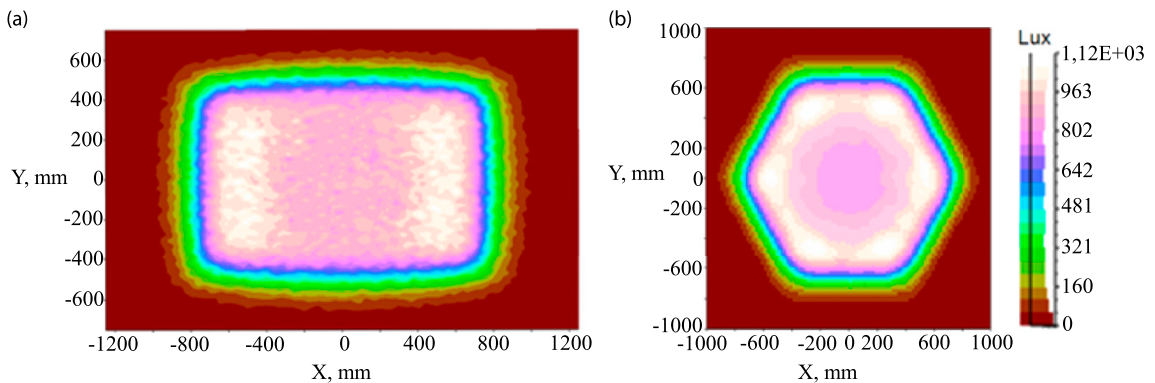
Figure 6   Light distributions on a receiver plane of CoB white LED integrated with different geometries of freeform lenslet: (a) rectangle, (b) hexagon

Supplemental Figure 7. It clearly displays that a uniform illumination can be produced in a rectangular plane of 0.75 × 1.5 m located at a distance of 2 m away from the light source. The calculated efficiency and uniformity of illumination are 87% and 70%, respectively. This hence would be an interesting piece in an 'off-axis lighting' spirit.

4. Results

To assess the aforementioned lighting system design, we implemented a proof-of-concept system with the structural parameters as shown in Table 1. The system was subsequently tested with a 10W CoB LED (Epileds Chip GT-P25W-XX). We collimated the light rays using the TIR collimator (Led-ink Optics Inc, 75 mm diameter). We finally used the freeform lenslet array, made of PMMA, where the collimated light could be redistributed to become uniform in an illumination region. The logical design of freeform lenslet array is the same diameter as the TIR collimator, that is, 75 mm. Figure 7(a)–(d) show the separate components and the entire LED luminaire.

To evaluate the feasibility of using flexible design of lenslet shape for producing various illumination shapes, we designed here two free-form lens arrays consist of square and rectangle lenslet. The results with other shapes could be deduced based on the principle proposed in our design that would be indeed needless for our central claims here. The freeform lens arrays in this design were manufactured by the computerised numerical control (CNC) moulding method. The typical procedure is as follows: a 3D model was drawn using AutoCAD according to the structure parameter determined as the simulation

data. Next, the 3D drawing was converted to G-code output of the Aspire software to communicate with the CNC machine. The moulding stage was then processed to render a flat PMMA film to a freeform lenslet array. The thickness and diameter of the as-fabricated freeform lenslet array were 5 and 75 mm, respectively. The resolution of the CNC machine used in this work is 20 μm. The polishing process was finally implemented to prevent the surface imperfections may be caused in the moulding stage, which can induce the attenuation of the collection efficiency of the freeform lens array. Other detail of the manufacturing process can be seen in Ref. 19.

Supplemental Figure 8 shows the freeform lens arrays after polishing for two shapes of lenslet (square and rectangle). The distance from the light source to the illumination area was kept at 2 m for both configurations. The corresponding light distribution on the receiver plane is present in Figure 8(a) and (b). The illumination surfaces of square and rectangle area have the sizes of 1.5 × 1.5 m and 1.2 × 1.8 m, respectively. It clearly shows that the obtained radiation patterns have the same geometry as the shape of the corresponding lenslet.

To assess precisely the degree of uniformity of the radiation pattern generated by two above lenslet arrays, the illumination was captured and analysed using a photodiode (Vishay semiconductors, BPW34) counts, associated with an 8-bit digitisation scheme giving a range of 0–255. We consider a pixel area, say 2 × 2 m (see Figure 8(c) and (d)), and the other experimental conditions for the system were similar to the simulation study. The uniformity of the obtained radiation pattern was experimentally determined to be 75% at hand, close to those of the simulation results displayed in Figures 5(b) and 6(a), so it brackets rather expected value in our case. It is likely that the difference between the real and ideal system assumed in the simulation results from the surface defect may be caused during the moulding process. We can therefore conclude that, on this basis, the proposed technique shows the immense gains especially in term of multiple
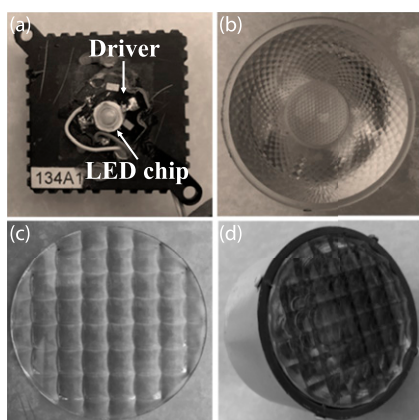
Figure 7   Photographs of (a) LED chip, (b) TIR collimator, (c) freeform lenslet array and (d) LED luminaire

Receiver plane

LED luminaire
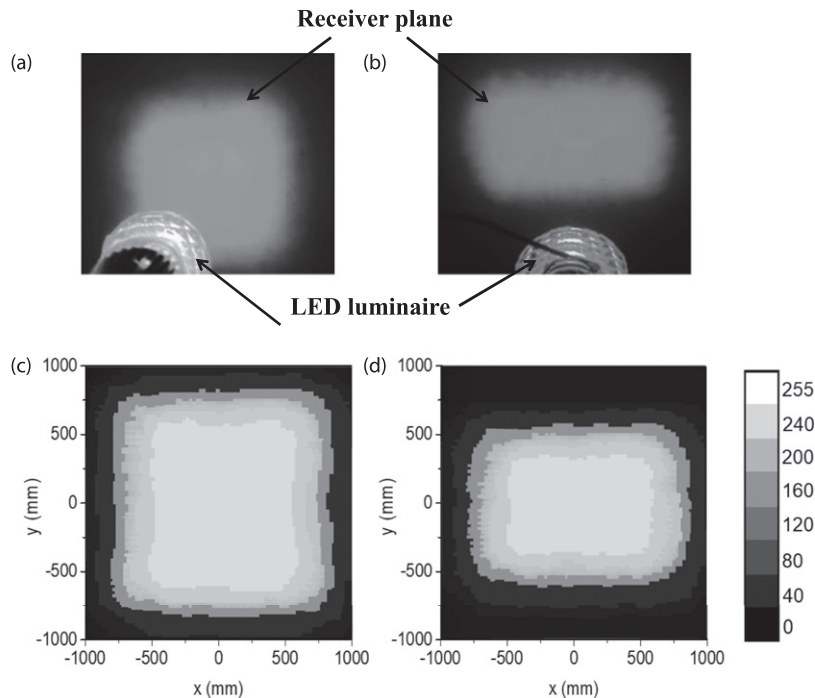
Figure 8 Light performances of CoB white LED integrated with (a) a TIR collimator + a square lenslet array and (b) a TIR collimator + a rectangular lenslet array. Light distributions of CoB white LED integrated with (c) a TIR collimator + a square lens arrays and (d) a TIR collimator + a rectangular lens arrays, counted with a photodiode and plotted by Matlab software

illumination patterns and a compact design of optical components.

5. Discussion

We expect that the proposed system (TIR collimator + freeform lenslet array) itself is suitable for the possible application in indoor lighting. We here indeed simulated the performance of the proposed lighting system in standard conditions of a virtual classroom. One such room with the dimensions of $8 \times 5 \times 3$ m was designed using Dialux. The 3D layout of the room's interior is shown in Figure 9. To preserve sufficient illumination, the initial input requirement was chosen including luminous flux per unit area of 500 lux, uniformity of above 70% for a room area of 40 m².[27,28] The light performance was calculated at the distance of 2.5 m away from the light source, whereas the other design parameters were similar to the study in sections 3 and 4. This distance ensures that there is a uniform illumination on the working table, as illustrated in Figure 9. A proper number of the luminaire was installed at the ceiling to grant a sufficient luminous for the room. We here selected the two most common types of LED luminaires, i.e., panel and parabolic downlight as shown in Supplemental Figure 9(a) and (b), respectively, for comparison with our proposed design. Technically, the LED panel makes use of a diffuser to grant an illumination more uniform compared to the use of the LED parabolic downlight. Still, this not only will increase the expense but also will attenuate the optical efficiency, typically involving the inevitable optical

loss of the diffuser, around 15–30%.[29] We designed a simulation of those LED luminaires based on the specifications of the LED panel light (Philips, SM400 C LED 36S)[30] and the LED downlight (VersaLux, VLP4).[31] We reasonable impose that the view angle of the panel and downlight is 24° and 180°, respectively.

We start our investigations by an evaluation of light performance on the working plane using a proposed luminaire, an LED panel luminaire and
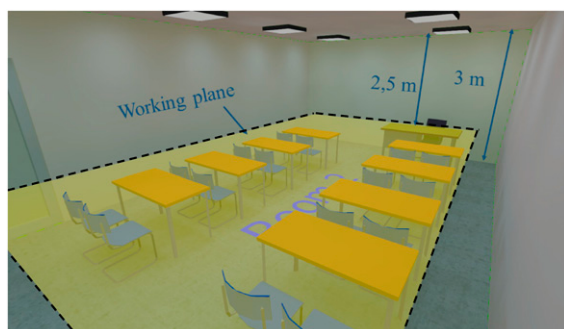
Figure 9 The visual 3D layout of the virtual classroom

an LED parabolic downlight luminaire. Figure 10(a)–(c) show the light distribution of the aforementioned luminaires on the working plane 2.5 m away from the light sources. We also plotted the luminous intensity, the inset in Figure 10(a)–(c), along the y-axis. Our proposed luminaire can produce a uniform illumination area of 1.5 × 1.5 m, as described earlier. Conversely, the downlight luminaire only created a narrow lighting area and gave rise a 'hot spot' in the centre of illumination area, thus it is suitable to illuminate for a specific area. For the panel luminaire, its light distribution was relatively uniform, mostly thanks to an inserted diffuser. However, clearly for this last case, the luminous efficiency was relatively weak, this would lead to the possibility of high power consumption (a corresponding evaluation for this issue will be given below). Figure 10(d) and (e) are the corresponding angular intensity distributions.

The results exhibited that the view angle of our proposed luminaire and a commercial parabolic LED downlight was narrower than that of LED panel. In a given context of indoor lighting, the
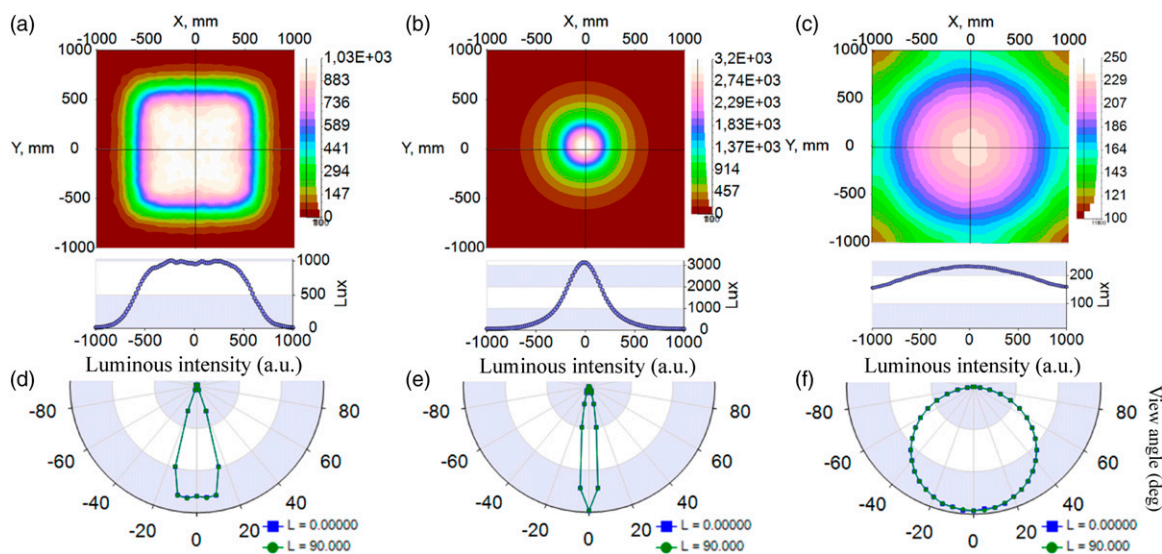
Figure 10 Light intensity distribution of (a) a proposed luminaire, (b) a commercial LED parabolic downlight and (c) a commercial LED panel. Inset shows a corresponding line chart along y-axis. Angular intensity distribution of (d) a proposed luminaire, (e) a commercial LED parabolic downlight and (f) a commercial LED panel

panel luminaire will launch a portion of the light to the room's walls, which thus may cause wasting energy and reducing lighting quality in the lighting area of interest. Hence, we can hope that highly uniform radiation provided by our proposed luminaire will fit with the indoor lighting, in order to help in addressing the major bottlenecks of both downlight and panel luminaire and will be discussed in detail below.

Of great interest in the feasibility of a lighting system, we now show a full test in a virtual classroom to evaluate the light performances that can be attained and the energy consumption issue for all studied lighting system. Table 3 presents a comparison of the initial conditions and optical performance between three types of luminaires, including our proposed luminaire, LED downlight luminaire and LED panel luminaire. To retain a roughly equal luminous flux on the working plane, our proposed design only needed to use 12 luminaires, compared to the use of 20 luminaires in an LED parabolic downlight system. Clearly, this can strongly reduce the material and installation costs. The increase of LED downlight luminaire well above the number of our proposed luminaire has implemented because the illumination area of the proposed luminaire is much uniform than that of a commercial LED downlight luminaire, as indicated in Figure 10(a) and (b). It is also expected that our proposed design consumes the lower electric power, compared to commercial LED panel counterpart, as seen in electric power consumption for the entire studied lighting system (Table 3). Our interpretation is that a very large output angle of the panel LED, reaching to nearly 180°, will lose a significant amount of light to the room's wall. We now visualise what the light distribution looks like at a large area in a designed classroom, say $8 \times 5 \times 3$ m. The light distributions on the working plane using three aforementioned designs are shown in Figure 11(a)–(c), so that we grasp more clearly the light performance in a virtual classroom. The colour bar was kept the same for all cases to ease comparison. And overall, in our design, most of the light output from the source was delivered directly and distributed uniformly to the illumination area, as seen in Figure 11(a). Because of narrow light distribution in the sufficient plausibility of a Gaussian line-shape (see Figure 10(b)), the LED downlight luminaires thus produced a heterogeneous illumination on the working plane (see Figure 11(b)). Figure 11 (c) is the case using the LED panel luminaires, and we see that the light distribution was relatively uniform; however, an adverse factor is its large power consumption, associated with the said optical loss. We further assessed the points that are of importance for the actual lighting system: the delivery efficiency and the uniformity of the illumination area.

Table 3 Comparison of the initial conditions and the optical performances between our proposed LED luminaire, commercial LED parabolic downlight and LED panel

Comparison categories	Proposed luminaire	LED parabolic downlight	LED panel
Initial conditions			
Room dimensions (m)	$8 \times 5 \times 3$	$8 \times 5 \times 3$	$8 \times 5 \times 3$
Luminaire dimensions (mm)	$76 \times 76 \times 51$	$100 \times 100 \times 96$	$440 \times 440 \times 45$
Number of LED luminaire	12	20	8
Luminous flux of light source (lm)	21,740	24,000	25,600
Lumen efficacy (lm/W)	100	100	80
Electric power (W)	217	240	320
Optical performances			
Luminous flux on the working plane (lm)	18,515	21,072	18,705
Delivery efficiency (%)	85.1	87.8	73.1
Illuminance min/max (lux)	393/486	355/687	294/516
Average illuminance	462	570	459
Uniformity (%)	86	62	65
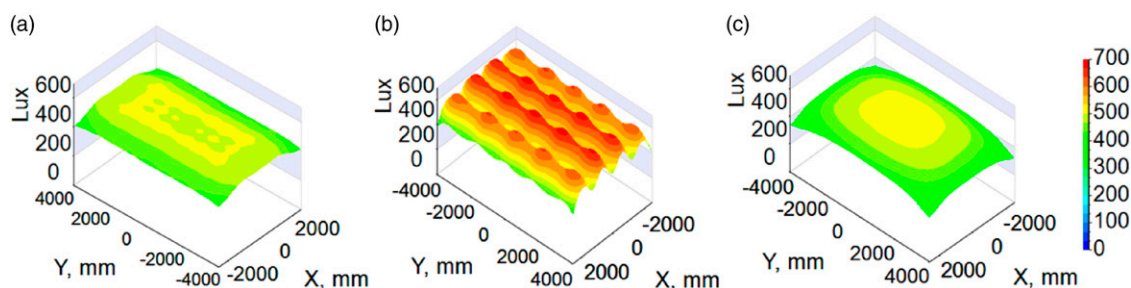
Figure 11   Light intensity distribution in a classroom, with a dimension of 8 × 5 × 3 m, of (a) our proposed luminaires, (b) commercial LED parabolic downlight luminaires and (c) commercial LED panel luminaires

From the data extracted from LightTools™ software, we define the delivery efficiency of light as the ratio of the luminous flux on the working plane and the luminous flux of the light source, and the corresponding values are listed in Table 3. Our proposed luminaires facilitated the high efficiency of light delivery, up to 85.0% compares well with existing methods. The difference between the minimum and the maximum illumination around the centre of the room using our proposed luminaire was only about 93 Lux, was much lower compared to that for downlight and panel, that is, 332 lux and 222 lux, respectively. Last but not least, the uniformity of the illumination area obtained from our proposed luminaire was 86%, which was better than that of the LED parabolic downlight and the LED panel. All things considered, using our proposed luminaire will have the advantage of saving electric power consumption and enhancing the uniformity of illumination in comparison with using commercial LED luminaires. It is therefore welcome for various lighting purposes, especially in the area of indoor lighting and street lighting, where have most often required a uniform illumination.

6. Conclusion

Herein, we have studied the LED lighting system with the task of producing highly uniform illumination. We first demonstrated that the wide angular distribution of LED light was redirected effectively to be collimating beam without negligible spatial spreading. A conventional distributor often possesses a very delicate design and requires distinct geometry for each element. To circumvent this, we have proposed a simple design of the distributors consisting of an array of the identical plano-convex lenslet. From the observation of light distributions entering a receiver plane, we have succeeded to produce a uniform illumination pattern. To evident this, we have analysed the performance of a real system and shown that it was equivalent to that of the simulation model. In addition, we take advantage of the versatile design of lenslet elements to alter the radiation shapes. For instance, the experimental demonstration of the square and rectangle illumination patterns was also shown. In addition, the off-axis lighting was well exemplified by modifying the focal point of lenslet elements. In a quest for an indoor lighting test, we showed a comparison with the commercial LED downlight and panel, which indicate the great potential of our proposed luminaire to be the alternative candidate for traditional LED light sources. Our strategy holds for great illumination performance as well as energy and cost-saving. Such a simple design is expected to enable the ubiquitous, inexpensive and high-performance lighting system, which is likely to deploy for niche lighting purposes.

Acknowledgements

Declaration of conflicting interests

The authors declared no potential conflicts of interest with respect to the research, authorship, and/or publication of this article.

Funding

ORCID iD

DT Vu ⓘ https://orcid.org/0000-0002-5651-3337

Supplemental material

Supplemental material for this article is available online.

References

1 Zeng X-Y, Yang L, Zhou X-T, Zhang YA, Chen EG, Guo TL. Pixel arrangement optimization of two-dimensional light-emitting diode panel for low-crosstalk autostereoscopic light-emitting diode displays. *Optical Engineering* 2017; 56: 063104.

2 Won Y-Y, Yoon SM, Seo D. White LED-based optical wireless link with improved transmission capacity using nonorthogonal multiamplitude phase frequency modulation. *Optical Engineering* 2017; 56: 066103.

3 Daskalakis KS, Freire-Fernández F, Moilanen AJ, van Dijken S, Torma P. Converting an organic light-emitting diode from blue to white with Bragg modes. *ACS Photonics* 2019; 6: 2655–2662.

4 Cao M, Xu Y, Li P, Yang D, Zhang Q. Recent advances and perspectives on light emitting diodes fabricated from halide metal perovskite nanocrystals. *Journal of Materials Chemistry C* 2019; 7: 14412–14440.

5 Choi MK, Yang J, Hyeon T, Kim DH. Flexible quantum dot light-emitting diodes for next-generation displays. *NPJ Flexible Electron* 2018; 2: 10.

6 Nardelli A, Deuschle E, de Azevedo LD, Pessoa JLN, Ghisi E. Assessment of light emitting diodes technology for general lighting: A critical review. *Renewable and Sustainable Energy Reviews* 2017; 75: 368–379.

7 Shi H, Zhu C, Huang J, Chen J, Chen D, Wang W, et al. Luminescence properties of YAG: Ce, Gd phosphors synthesized under vacuum condition and their white LED performances. *Optical Materials Express* 2014; 4: 649–655.

8 Wang K, Wu D, Qin Z, Chen F, Luo X, Liu S. New reversing design method for LED uniform illumination. *Optics Express* 2011; 19: A830–A840.

9 Wang K, Chen F, Liu Z, Luo X, Liu S. Design of compact freeform lens for application specific light-emitting diode packaging. *Optics Express* 2010; 18: 413–425.

10 Sun L, Jin S, Cen S. Free-form microlens for illumination applications. *Applied Optics* 2009; 48: 5520–5527.

11 Su Z, Xue D, Ji Z. Designing LED array for uniform illumination distribution by simulated annealing algorithm. *Optics Express* 2012; 20: A843–A855.

12 Moreno I, Sun CC. Modeling the radiation pattern of LEDs. *Optics Express* 2012; 16: 1808–1819.

13 Ding Y, Liu X, Zheng Z-R, Gu PF. Freeform LED lens for uniform illumination. *Optics Express* 2008; 16: 12958–12966.

14 Oliker VI. Differential equations for design of a freeform single lens with prescribed irradiance properties. *Optical Engineering* 2014; 53: 031302.

15 Benítez PG, Minano JC, Blen J, Arroyo RM, Chaves J, Dross O, et al. Simultaneous multiple surface optical design method in three dimensions. *Optical Engineering* 2004; 43: 1489–1502.

16 Ma D, Feng Z, Liang R. Freeform illumination lens design using composite ray mapping. *Applied Optics* 2015; 54: 498–503.

17 Wang G, Wang L, Li F, Kong D. Design of optical element combining Fresnel lens with microlens array for uniform light-emitting diode lighting. *Journal of the Optical Society of America A* 2012; 29: 1877–1884.

18 Vu N, Pham T, Shin S. LED uniform illumination using double linear Fresnel lenses for energy saving. *Energies* 2017; 10: 2091.

19 Vu H, Kieu NM, Gam DT, Shin S, Tran QT, Vu NH. Design and evaluation of uniform LED illumination based on double linear Fresnel lenses. *Applied Sciences* 2020; 10: 3257.

20 Aslanov E, Doskolovich LL and Moiseev MA. Thin LED collimator with free-form lens array for illumination applications. *Applied Optics* 2012; 51: 7200–7205.

21 Aslanov E, Doskolovich LL, Moiseev MA. Designing of slim optics for prescribed light patterns. *Computer Optics* 2012; 36: 227–234.

22 Song I-H, Park T. PMMA solution assisted room temperature bonding for PMMA-PC hybrid devices. *Micromachines* 2017; 8: 284.

23 Vu DT, Vu H, Vu NH. A homogeniser inspired by the crustacean's eye with uniform irradiance distribution and high optical efficiency characteristics for concentrated photovoltaics system. *Solar Energy* 2021; 221: 87–98.

24 Vu DT, Vu H, Shin S, Tran QT, Vu NH. New mechanism of a daylighting system using optical-fiber-less design for illumination in multi-storey building. *Solar Energy* 2021; 225: 412–426.

25 Cree LED. XLamp XB-D. Durham, NC: Cree LED. Retrieved from https://www.cree.com/led-components/products/xlamp-leds-discrete/xlamp-xb-d (accessed 25 August 2020).

26 Cree LED. CXA LES Arrays. Durham, NC: Cree LED. Retrieved from https://www.cree.com/led-components/cxa on (accessed 25 August 2020).

27 Illumination Engineering Society. *Lighting Handbook: Reference and Application*. 10th Edition. New York, NY: Illumination Engineering Society, 2011.

28 Vu N-H, Pham T-T, Shin S. Modified optical fiber daylighting system with sunlight transportation in free space. *Optics Express* 2016; 24: A1528–A1545.

29 Wang K, Liu S, Luo X, Wu D. *Freeform Optics for LED Packages and Applications*. Singapore: John Wiley & Sons, 2017.

30 Philips Lighting. *Slim Blend Square Surface Mounted*. Amsterdam, Netherlands: Philips Lighting. Retrieved from https://www.assets.signify.com/is/content/PhilipsLighting/fp910500459962-pss-global (accessed 3 September 2020).

31 Starfire Lighting Inc. *LED Perimeter Slot*. Wood-Ridge, NJ: Starfire Lighting Inc. Retrieved from http://www.starfirelighting.com/led_28.php (accessed on 3 September 2020)